Biophysical Chemistry 146 (2010) 133–137

Contents lists available at ScienceDirect

Biophysical Chemistry

journal homepage: http://www.elsevier.com/locate/biophyschem

Quantifying the membrane potential during *E. coli* growth stages

Corina Teodora Bot *, Camelia Prodan

New Jersey Institute of Technology, Physics Department, Tiernan Hall, 161 Warren Street, Newark, NJ 07102, USA

ARTICLE INFO

Article history:
Received 10 October 2009
Received in revised form 20 November 2009
Accepted 20 November 2009
Available online 30 November 2009

Keywords:
Escherichia coli
Dielectric spectroscopy
Impedance analysis
Membrane potential

ABSTRACT

The presence of the resting membrane potential has a strong effect on the dielectric behavior of cell suspensions. Using this observation and a well-established theoretical model, the low frequency dielectric dispersion curves of *E. coli* cell suspensions are de-convoluted to obtain the resting membrane potential of *E. coli* cells at various growth stages. Four regions of the exponential growth stage are investigated and the measurements indicate that the membrane depolarizes from −220 mV in the early exponential phase to −140 mV in the late exponential phase. The conductivity of the cell suspension is also found to decrease as the cells progress from the early to the late exponential phases.

1. Introduction

In the microbial universe, chemiosmotic reactions across the cell membrane regulate the flow of nutrients and metabolites, the ATP synthesis and the pH level inside the cells. The ion transport across the cell membrane is metabolically regulated and one expects distinct variations during the metabolic cycle of the intrinsic cell parameters, like the resting membrane potential, but also of the medium supporting the growth of the microorganisms. Impedance spectroscopy (IS) is an experimental technique that measures the cumulative effect of all these changes on the electrical impedance of a macroscopic sample [1].

One goal in impedance spectroscopy is to de-convolute the impedance measurements and obtain separate quantitative information about the intrinsic cell parameters, on one hand, and about the medium, on the other hand [2–7]. Other techniques, such as patch clamping, can be used to measure the intrinsic cell parameters, but such techniques are very often invasive or have to be performed in a lab under a microscope. In contradistinction, IS can monitor fast changes and the measurements can be recorded with a simple impedance probe in quite various conditions.

Due to a sustained effort from a broad scientific community, the de-convolution of the IS measurements is becoming a reality [7–16]. Past theoretical studies predicted that one key to such de-convolution is to be found in the very low frequency impedance data [17,18]. A microscopic theoretical model for the macroscopic dielectric response of cells in suspension, to be discussed shortly, predicts a great sensitivity of the macroscopic dielectric function to the intrinsic cell parameters, in the frequency range below 10 kHz. This observation, together with the explicit theoretical model, provides a venue for de-convoluting the IS measurements, which is explored in this work. On a second front, the experimental IS measurements in the very low frequency range are becoming more and more precise. In particular, one of our recent works showed good correlations between the IS experimental data and the theoretical predictions [19]. The values of the resting membrane potential obtained by de-convoluting the IS data were found to be in good agreement with the values obtained by more traditional methods.

The present work gives a quantitative characterization of several intrinsic cell parameters during the *E. coli* metabolic cycle. It is shown that IS measurements can distinguish between different life stages of *E. coli*. It is also shown that the experimental dielectric dispersion curves can be fitted well by the theoretical model. Several parameters entering the model are fixed to values obtained by direct measurements, and other parameters, like the resting membrane potential, are left as fitting variables. Our de-convoluted data show that the resting membrane potential may hyperpolarize to a value of −220 mV when *E. coli* are in the early exponential phase and may monotonically depolarize to −140 mV as *E. coli* enters the late exponential phase.

2. Materials and methods

2.1. The theoretical model

For simplicity, we use the theoretical model put forward in Ref. [17] which provides an analytical solution for spherical cells. According to this model, the dielectric response of living cells, in the frequency range below 10 MHz, is determined by the polarization of the ion charge distributions near the cells' membranes and by the dielectric composition of the cells. When an electric field is applied,

* Corresponding author. Tel.: +1 973 596 5865.
E-mail addresses: corina.bot@njit.edu (C.T. Bot), cprodan@adm.njit.edu (C. Prodan).

0301-4622/$ – see front matter © 2009 Elsevier B.V. All rights reserved.
doi:10.1016/j.bpc.2009.11.005

the ionic distributions around the cell membranes are deformed and large dipole moments are created, leading to extremely strong collective dielectric response of the cells in solutions. This phenomenon is known as the alpha effect, and it appears only at low frequencies, typically below 10 kHz. As the frequency is increased, there is a sharp threshold above which the ions can no longer follow the electric field and the alpha effect disappears. The dielectric response enters the so-called beta regime, which is entirely determined by the dielectric composition of the cells. The dielectric response in the alpha regime is directly proportional to the concentrations of the ionic charge accumulated around the membrane, which in turn are directly proportional to the resting membrane potential.

The alpha and beta regimes have been quantified using a set of coupled equations, which take into account the diffusion of charges along the surface of the membrane and the dielectric composition of the cell [17]. In the present work, we use an explicit analytic solution of this model, obtained in Ref. [18], which provided the following formula for the complex dielectric function $\varepsilon^*=\varepsilon+\sigma/j\omega$ of a solution with cells:

$$\varepsilon^*(\omega)=\varepsilon_0^*\left[1-\frac{p\alpha(\omega)}{1-p\alpha(\omega)/3}\right], \tag{1}$$

where $\alpha(\omega)$ is the polarizability of the individual cells:

$$\alpha(\omega)=\frac{6\lambda}{3-\lambda}\left[1-\frac{\Delta V\frac{2R_2\varepsilon_1}{3d\varepsilon_{vac}}}{\left(1+\frac{j\omega R_2^2}{2D}\right)(3-\lambda)(\varepsilon_{10}^*+\varepsilon_0^*)+\Delta V\frac{2R_2\varepsilon_1}{3d\varepsilon_{vac}}}\right];$$
$$\lambda=\frac{\varepsilon_2^*-\varepsilon_1^*}{\varepsilon_2^*+\varepsilon_1^*};\ \varepsilon_{10}^*=\varepsilon_1^*\left\{1-\frac{3}{1-\left(\frac{R_1}{R_2}\right)^3\frac{\varepsilon_2^*+2\varepsilon_1^*}{\varepsilon_2^*-\varepsilon_1^*}}\right\} \tag{2}$$

The independent input parameters entering the formula are: the volume fraction p of the cell solution, the outer and inner average radius of the cell's membrane, R_1 and R_2 ($d=R_1-R_2$; consideration of a strict ellipsoidal shape for the cells makes very little difference [20,21]), the complex dielectric function of the medium $\varepsilon_0^*=\varepsilon_0+\sigma_0/j\omega$, of the membrane $\varepsilon_1^*=\varepsilon_1+\sigma_1/j\omega$ and of the inner cell region $\varepsilon_2^*=\varepsilon_2+\sigma_2/j\omega$; the diffusion constant D of surface charges accumulated around the membrane and the resting membrane potential ΔV.

2.2. Experimental methods

E. coli K12 wild type (www.atcc.com) were incubated in 10 ml of Tryptone Soy broth (growth media) at 175 rpm and 37°C to the saturation phase for 16 h. Afterwards, 1 ml of this solution was re-suspended in 39 ml of media and incubated in the same conditions. During this incubation, the growth stages were correlated with the optical density (OD) and the growth curve was generated. The OD measurements were recorded every 15 min at 600 nm with a Genesys 10vis spectrophotometer from Thermo Electron Corporation. Equal amounts of cells and media, from another overnight culture, were re-suspended and incubated in different sterile tubes and later harvested when the ODs reached 0.2, 0.3, 0.4, 0.6, 0.8, 1 and 1.1. Once the cells in a tube reached the desired OD, they were further prepared for the IS measurements. For this, the tubes were centrifuged at 2522×*g* for 6 min and the pellet was re-suspended in ultra-pure water (Milli-Q Direct Q water system) with 5 mM glucose to an OD_{600} of 0.301, ±0.004. Therefore, we prepared seven equal OD_{600} aqueous solutions of *E. coli* in different growth stages. These solutions were further characterized by IS measurements. The geometrical parameters of the cells were measured by imaging the cells of each solution at 100× magnification and analyzing the pictures taken with a CCD camera (Sensicam qe The Cooke Corporation) attached to a Zeiss Axiovert 200 inverted microscope.

For IS measurements, we used the experimental setup described in Refs. [19,22]. The solution to be measured is placed between two parallel gold-plated electrodes that are enclosed in a cylindrical glass tube. The radius of the electrodes was $R=28.1$ mm. The distance between the electrodes was $l=3.1$ mm and the applied voltage was 0.15 V, generating low electric fields of approximately 0.5 V/cm. The complex impedance Z of the measuring cell was measured using a Solartron 1260 Impedance Analyzer over the frequency range from 200 Hz to 1 MHz. The cleaning procedure of the measuring cell consists of washing with water for approximately 1 min followed by a three times rinse with DI water for both the chamber and the electrodes. After the rinse, it is made sure that a measurement on DI water gives dielectric parameters that are consistent with the standard values of the DI water.

If the measured impedance Z were equal to the intrinsic impedance Z_s of the sample, the complex dielectric function $\varepsilon^*=\varepsilon+\sigma/j\omega$ of the cell suspension could be calculated from: $\varepsilon^*(\omega)=\frac{l/\pi R^2}{j\omega Z}$. Unfortunately, all low frequency IS measurements are affected by the polarization effect. This effect is due to the polarization of the double layer of charges appearing at the contact between the solution and electrodes. As a result, the measured impedance Z is actually a sum of the intrinsic impedance of the sample and the impedance of the polarization layers: $Z=Z_s+Z_p$. An efficient method for correcting the polarization effect was developed in Refs. [23,24], which we also follow here. It consists of the following steps:

i) Record the impedance $Z(\omega)$ of the measuring cell for frequencies between 200 Hz and 1 MHz.
ii) Using gentle centrifugation (2522×*g* for 6 min), separate the medium in which the cells were suspended.
iii) Perform an IS measurement on the medium and record $Z_m(\omega)$ for frequencies between 200 Hz and 1 MHz.
iv) In the frequency range above 10 kHz, where the polarization effect is absent, fit $Z_m(\omega)$ data with the expression $Z_{ideal}(\omega)=\frac{l/\pi R^2}{j\omega\varepsilon_0+\sigma_0}$, to obtain the dielectric permittivity ε_0 and conductivity σ_0 of the medium.
v) Compute the polarization impedance from $Z_p=Z_m-Z_{ideal}$, where Z_{ideal} is computed with ε_0 and σ_0 obtained from the previous fit.
vi) Obtain the intrinsic impedance of the cell solution from $Z_s=Z-Z_p$.
vii) Compute the sample's dielectric function from $\varepsilon^*(\omega)=\frac{l/\pi R^2}{j\omega Z_s}$.

The protocol for correcting the polarization effect was extensively analyzed and tested in Ref. [23] and was subsequently applied in Ref. [19] to obtain accurate dielectric measurements on *E. coli* cell suspensions.

3. Results

Fig. 1a shows the growth curve of *E. coli*, presented as a plot of OD_{600} versus time. All three stages of growth are observed: lag (in the first 60 min), exponential (60–240 min) and stationary (240–300 min). Fig. 1b shows a plot of the conductivity σ of the *E. coli* cell solution at different growth stages. The conductivity was measured at 1031 Hz. The plot is presented not as function of time, but of the corresponding OD. To aid the reading, the same colors and symbols were used in Fig. 1a and b. We found that σ as function of OD, obeys quite accurately an exponential. The continuous line in Fig. 1b represents a fit with the equation $y=0.014\times e^{-2.29x}$, which yielded an R-value of 0.99.

Fig. 2 illustrates how the polarization error was corrected (OD = 0.667 was chosen for this example). The data marked by the red circles represent the imaginary part of the measured impedance $Z(\omega)$ of

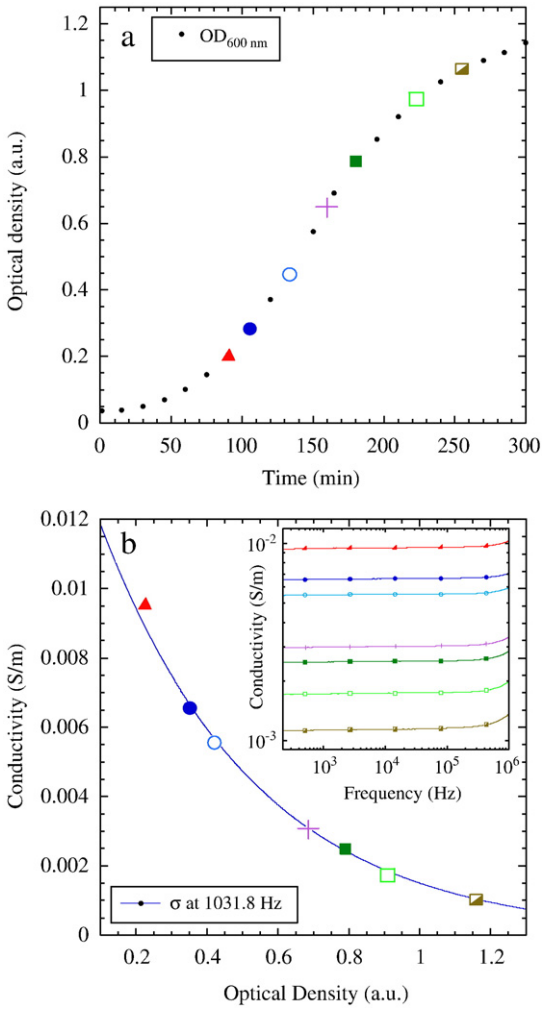

Fig. 1. (a) *E. coli* growth curve: dependence of optical density ($OD_{600\,nm}$) on cell age. Symbols represent cells ages (ODs) at which they were harvested for measurements: 0.231 (▲), 0.352 (●), 0.409 (○), 0.684 (+), 0.793 (■), 0.913 (□), 1.149 (◪). After harvesting the cells at above ODs, each sample was diluted or concentrated to OD 0.3 for dielectric spectroscopy measurements. (b) Conductivity at 1031.8 Hz computed from dielectric measurements as a function of cell age. Symbols represent cells ages (ODs) at which they were harvested for measurements: 0.231 (▲), 0.352 (●), 0.409 (○), 0.684 (+), 0.793 (■), 0.913 (□), 1.149 (◪) and then all diluted or concentrated to OD 0.3. The inset presents conductivity data computed from impedance recordings vs. frequency.

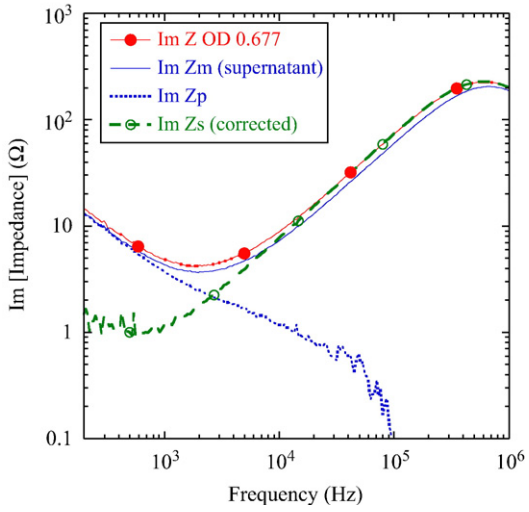

Fig. 2. Imaginary parts of impedances: cell suspension (●), supernatant (Im Z_m, solid line), polarization error (Im Z_p, dashed line) and corrected cells after polarization removal (Im Z_s, ○) plotted as a function of frequency.

the measuring cell containing the cells in suspension. The full blue line represents the imaginary part of the impedance of the medium $Z_m(\omega)$. For all IS measurements, $Z_m(\omega)$ is fitted with the expression of $Z_{ideal}(\omega)$ presented in the previous section. The fitting was restricted to the frequencies above 1 kHz, where the polarization effect is negligible. This is inferred from the *R*-values of 0.99 or better for this fittings, which shows that $Z_{ideal}(\omega)$ is indeed a very good characterization of $Z_m(\omega)$. The fitted values of the conductivity σ_0 of the medium are similar to the ones presented in Fig. 1b, with a fitting error below 0.01%, while for ε_0 the fitting error was below 0.1%. These values represent an average over three independent measurements (the entire protocol has been repeated three times, in different days).

After we obtained ε_0 and σ_0 of the medium, we performed the polarization removal as explained in the previous section and exemplified in Fig. 2. From the intrinsic impedance Z_s, we computed the dielectric function and the conductivity of the cell suspensions, which are shown in Fig. 3a and b. The curves correspond to different growth stages: OD 0.2, OD 0.3–0.4, OD 0.6 and OD 0.8–1, and were obtained by averaging over three independent measurements. The plots also present the standard error for these three independent measurements. Here, the cells are measured at the same concentration; the OD notation is used only to present the growth stages.

Fig. 3 shows large variations in the dielectric response of the cell suspensions for different growth stages. We correlated these variations with the changes in the membrane potential. The theoretical formulas shown in Eqs. (1) and (2) were used to fit the experimental dispersion curves shown in Fig. 3 and obtain the resting membrane potential of *E. coli* for the corresponding growth stages. The following parameters were fixed during the fitting: the volume fraction $p = 0.02$ and the average cell radius of 1.35 μm for ODs 0.2, and 1.5 μm for all other ODs. Both the volume fraction and radius were obtained based on microscope images of cells. The diffusion coefficient $D = 2.3 \times 10^{-7}$ m^2/s [19] (adjusted to best fit the data); the effective dielectric constant of the membrane $\varepsilon_1 = 40$; the dielectric constant $\varepsilon_2 = 78$ and conductivity $\sigma_2 = 0.2$ S/m of the intracellular medium, (taken from Ref. [9]); the thickness of the *E. coli* inner membrane, $d = 5$ nm (taken from Ref. [25]). The membrane potential was left as a fitting parameter. A hyperpolarized resting membrane potential of −220 mV is obtained for cells in the early exponential phase (OD 0.2). This value decreases to −200 mV for ODs 0.3−0.4, and to −160 mV for OD 0.6. As the cells enter the late exponential phase, ΔV settles at −140 mV (ODs 0.8–1). Fig. 4 presents a comparison between the theoretical and experimental curves.

4. Discussion

As cells are harvested from their growth media and re-suspended in purified water with 5 mM glucose, their cytoplasmic membranes serve mainly as energy transmitters and their proton pumps enhance transport since cells undergo demanding circumstances. This effect is due to depravation of cells of growth media nutrients, and it creates a larger ionic transport across their membranes. As a result, the cells modify the conductive properties of the medium. The data from Fig. 1b shows that more ions are released in the medium when cells are collected in the early growth stage. This observation is in agreement with our later finding that the cells have a hyperpolarized membrane potential in the early growth stage. The dielectric constants ε_0 and conductivities σ_0 of the medium corresponding to the three independent measurements are very close. This demonstrates that the polarization removal procedure is stable and the experiments are repeatable. We would also like to comment that the measurements shown in Fig. 3(a–b) were performed on three independent cultures. The error bars in Fig. 3(a–b) indicate that the

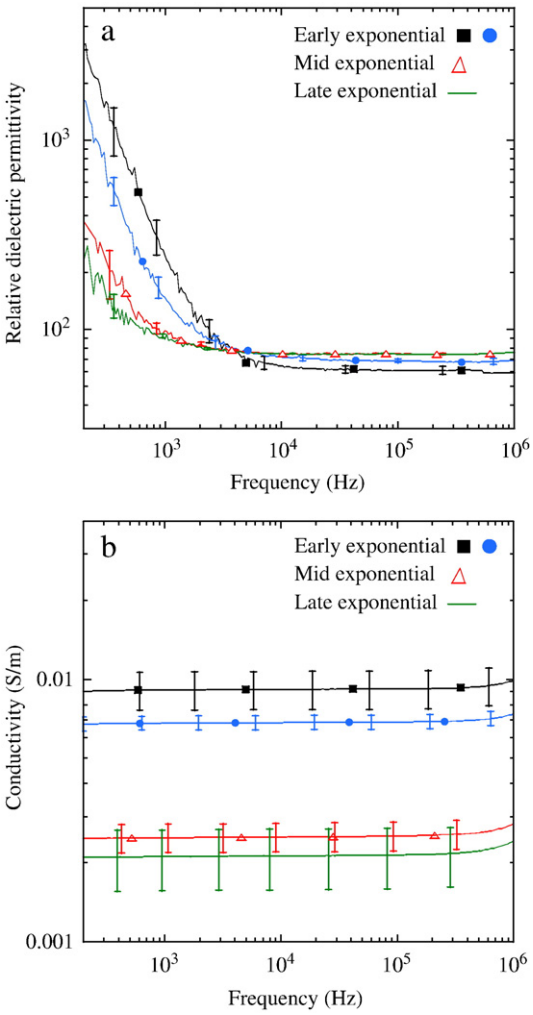

Fig. 3. (a) Relative dielectric permittivity of suspensions with the same *E. coli* concentration but harvested at ODs: 0.2 (■), 0.3–0.4 (●), 0.6 (△), 0.8–1 (solid line). As cell age increases, relative dielectric permittivity decreases. (b) Conductivity of cell suspensions with the same *E. coli* concentration but cells harvested at ODs: 0.2 (■), 0.3–0.4 (●), 0.6 (△), 0.8–1 (solid line). As cell age increases, conductivity decreases.

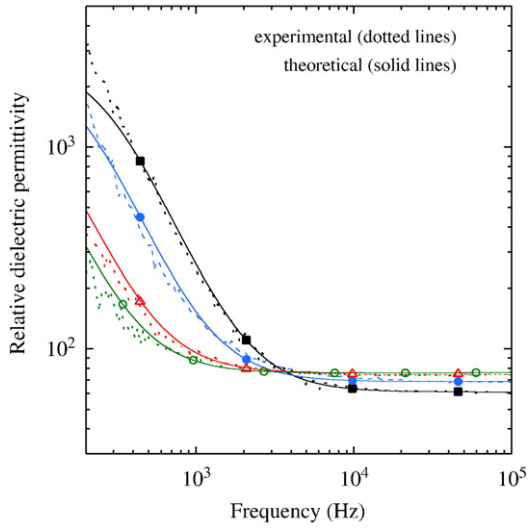

Fig. 4. Relative dielectric permittivity of *E. coli* for membrane potential: −220 mV (■), −200 mV (●), −160 mV (△), −140 mV (○): theoretical fittings (solid lines) and experimental results (dotted lines).

IS measurements can, indeed, distinguish between the different growth stages of *E. coli*.

Previous studies [26–29] of the intracellular cation concentrations established that the concentrations are functions of the age of the culture, the pH of the medium and the accumulation of metabolic products. Same studies found that the K^+ concentration falls and the Na^+ concentration rises as the culture is aging. In line with these observations, we observe that, as cells go from early exponential phase (OD 0.2) to the mid exponential (OD 0.6) and further on to the late exponential phase (OD 1), there is a continuous decrease in the low frequency dielectric permittivity (see Fig. 3 a). It is a fact that the intracellular K^+ concentration in *E. coli* exceeds that of the external medium [28,29] and, since K^+ is more concentrated inside the cells, a net ionic movement from inside out should be established when cells are re-suspended in water, until a new equilibrium membrane potential is reached. The larger the original K^+ inside the cell, the more K^+ is released in water. According to these arguments, the conductivity of the cell solutions and of the supernatant should decrease as *E. coli* pass from one growth stage to the other. This effect is easily observable in Figs. 1b and 3b.

The experimental observations for the high frequency dielectric permittivity vary in the literature. One reference [30] finds ε between 70 and 74 for suspensions of ellipsoidal cells. For *E. coli* in culture medium, Ref. [31] finds ε between 92 and 95 at 5 MHz and Ref. [9] finds a value closed to 100.

E. coli cells have two membranes separated by a cell wall in between. The inner membrane acts as the permeability barrier while the outer membrane and cell wall provide additional protection [32]. The outer membrane is different from the ordinary lipid bilayers and is not regarded as a barrier for ions but as a filter for large molecules [9]. Because of these properties, only the inner membrane of *E. coli* was considered in the theoretical simulations. Previous studies [33] reported a ΔV of −150 mV for *E. coli* in suspensions, and similar values were reported in Ref. [34] from microelectrode recordings on single cells. This value is very close to $\Delta V = -140$ mV that we found for the *E. coli* cells harvested at late exponential phase.

5. Conclusions

IS measurements on *E. coli* harvested at different growth stages and re-suspended in aqueous solutions of equal concentrations show distinct features that can be correlated to the age of the cells. Using a microscopic model of the macroscopic complex dielectric functions, we de-convoluted the IS measurements and obtained direct information about the cell parameters and the medium. During this process, we found that the fitting between the theoretical curves and experiment is accurate.

From de-convolution we see that *E. coli* cells have a hyperpolarized membrane potential in the early growth stage, which we estimated to be −220 mV. As the cells age, the membranes depolarize and the membrane potential reaches a value of −140 mV in the stationary phase. This latter value was reported by patch clamping measurements in Ref. [34]. In line with these findings, we find that ion release into the aqueous solution is much stronger when the cells are in the early growth stage and that it becomes weaker as the cells age. This is directly reflected in the conductivity of the medium and of the cell suspension, which we were able to map quantitatively. Our findings support previous studies on the intracellular cation concentrations and can lead in the future to better quantitative models of the ion transport through the membrane.

References

[1] K. Foster, H.P. Schwan, Dielectric properties of tissues and biological materials: a critical review, Critical Reviews in Biomedical Engineering 17 (1) (1989) 25–104.
[2] P.C. Braga, M. Culici, M.D. Sasso, The post-antibiotic effects of rokitamycin (a 16-membered ring macrolide) on susceptible and erythromycin-resistant strains of

Streptococcus pyogenes, International Journal of Antimicrobial Agents 24 (2004) 56–62.
[3] P. Cady, et al., Electrical impedance measurements: rapid method for detecting and monitoring microorganisms, Journal of Clinical Microbiology 7 (3) (1978) 265–272.
[4] S.P. Kounavesa, et al., Microbial life detection with minimal assumptions, SPIE Proceedings 4495 instruments, methods, and missions for astrobiology, SPIE Proceedings 4495 Instruments, Methods, and Missions for Astrobiology, 2001.
[5] R.E. Madrid, C.J. Felice, Microbial biomass estimation, Critical Reviews in Biotechnology 25 (2005) 97–112.
[6] P.A. Noble, et al., Factors influencing capacitance-based monitoring of microbial growth, Journal of Microbiological Methods 37 (1999) 51–64.
[7] J.C.S. Richards, et al., Electronic measurement of bacterial growth, Journal of Physics E: Scientific Instruments 11 (1978) 560–568.
[8] K. Asami, E. Gheorghiu, T. Yonezawa, Real-time monitoring of yeast cell division by dielectric spectroscopy, Biophysical Journal 76 (1999) 3345–3348.
[9] W. Bai, K.S. Zhao, K. Asami, Dielectric properties of *E. coli* cell as simulated by the three-shell spheroidal model, Biophysical Chemistry 122 (2006) 136–142.
[10] W. Bai, K.S. Zhao, K. Asami, Effects of copper on dielectric properties of *E. coli* cells, Colloids and Surfaces B: Biointerfaces 58 (2007) 105–115.
[11] M. Ciureanu, W. Levadoux, S. Goldstein, Electrical impedance studies on a culture of a newly discovered strain of *Streptomyces*, Enzyme and Microbial Technology 21 (1997) 441–449.
[12] A. Di Biasio, C. Cametti, D-glucose-induced alterations in the electrical parameters of human erythrocyte cell membrane, Bioelectrochemistry (2009), doi:10.1016/j.bioelechem.2009.08.006.
[13] C.J. Felice, M.E. Valentinuzzi, Medium and interface components in impedance microbiology, IEEE Transactions on Biomedical Engineering 46 (12) (1999) 1483–1487.
[14] R.M. Lee, et al., Distinguishing between apoptosis and necrosis using a capacitance sensor, Biosensors and Bioelectronics 24 (2009) 2586–2591.
[15] L. Yang, Y. Li, Detection of viable *Salmonella* using microelectrode-based capacitance measurement coupled with immunomagnetic separation, Journal of Microbiological Methods 64 (2006) 9–16.
[16] A.M. Zhivkov, A.Y. Gyurova, High frequency electric polarizability of bacteria *E. coli*: dependence on the medium ionic strength, Colloids and Surfaces B: Biointerfaces 66 (2) (2008) 201–205.
[17] C. Prodan, E. Prodan, Dielectric behaviour of living cell suspensions, Journal of Physics D: Applied Physics 32 (3) (1999) 335–343.
[18] E. Prodan, C. Prodan, J.H. Miller, The dielectric response of spherical live cells in suspension: an analytic solution, Biophysical Journal 95 (9) (2008) 4174–4182.
[19] C. Bot, C. Prodan, Probing the membrane potential of living cells by dielectric spectroscopy, European Journal of Biophysics 38 (8) (2009) 1049–1059.
[20] A. Di Biasio, L. Ambrosone, C. Cametti, Numerical simulation of dielectric spectra of aqueous suspensions of non-spheroidal differently shaped biological cells, Journal of Physics D: Applied Physics 42 (2) (2008) 025401 (9pp).
[21] A. Di Biasio, C. Cametti, Effect of shape on the dielectric properties of biological cell suspensions, Bioelectrochemistry 71 (2) (2007) 149–156.
[22] C. Prodan, et al., Low-frequency, low-field dielectric spectroscopy of living cell suspensions, Journal of Applied Physics 95 (7) (2004) 3754–3756.
[23] C. Prodan, C. Bot, Correcting the polarization effect in the very low frequency dielectric spectroscopy, Journal of Physics D: Applied Physics 42 (2009) 175505 (10pp).
[24] H.P. Schwan, Alternating current electrode polarization, Biophysik 3 (1966) 181–201.
[25] V.R.F. Matias, et al., Cryo-transmission electron microscopy of frozen-hydrated sections of *Escherichia coli* and *Pseudomonas aeruginosa*, Journal of Bacteriology 185 (20) (2003) 6112–6118.
[26] W. Epstein, B.S. Kim, Potassium transport loci in *Escherichia coli* K-12, Journal of Bacteriology 108 (2) (1971) 639–644.
[27] O.V. Ignatov, et al., The electro-optical investigation of suspensions of *Escherichia coli* K-12 cells metabolizing glucose, lactose, and galactose, Microbiology 71 (3) (2002) 302–305.
[28] S.G. Schultz, A.K. Solomon, Cation transport in *Escherichia coli* — I. Intracellular Na and K concentrations and net cation movement, The Journal of General Physiology 45 (1961) 355–369.
[29] S.G. Schultz, N.L. Wilson, W. Epstein, Cation transport in *Escherichia coli*. II. Intracellular chloride concentration, The Journal of General Physiology 46 (1962) 159–166.
[30] C.M. Mihai, M. Mehedintu, E. Gheorghiu, The derivation of cellular properties from dielectric spectroscopy data, Bioelectrochemistry and Bioenergetics 40 (1996) 187–192.
[31] K.G. Ong, et al., Monitoring of bacteria growth using a wireless, remote query resonant-circuit sensor: application to environmental sensing, Biosensors and Bioelectronics 16 (2001) 305–312.
[32] J.M. Berg, J.L. Tymoczko, L. Stryer, Biochemistry, 5th Edition, 2002.
[33] D. Zilberstein, et al., *Escherichia coli* intracellular pH, membrane potential, and cell growth, Journal of Bacteriology 158 (1998) 246–252.
[34] H. Felle, et al., Quantitative measurements of membrane potential in *Escherichia coli*, Biochemistry 19 (15) (2009) 3585–3590.